Journal of Inflammation Research

Dovepress
Taylor & Francis Group

Open Access Full Text Article

ORIGINAL RESEARCH

Aging Inhibits Emergency Angiogenesis and Exacerbates Neuronal Damage by Downregulating DARS2

Dan Liu[1], Meilin Weng[2], Rui Wang[3], Wenchao Fu[1], Lijuan Zhang[1], Cheng Wang[4], Mingsen Liu[1], Tao Shen[1], Jirui Ren[1], Yinfei Song[1], Jiayu Li[1], Xianzhang Zeng[1,5]

[1]Department of Anesthesiology, The Second Affiliated Hospital of Harbin Medical University, The Heilongjiang Key Laboratory of Anesthesia and Intensive Care Research, Harbin Medical University, Harbin, People's Republic of China; [2]Department of Anesthesiology, Zhongshan Hospital, Fudan University, Shanghai, People's Republic of China; [3]Department of Critical Care Medicine, The Second Affiliated Hospital of Harbin Medical University, Harbin, People's Republic of China; [4]Department of Environmental Hygiene, School of Public Health, Harbin Medical University, Harbin, People's Republic of China; [5]Department of Anesthesiology, Chongqing University Affiliated Cancer Hospital, Chongqing, People's Republic of China

Correspondence: Xianzhang Zeng, Department of Anesthesiology, The Second Affiliated Hospital of Harbin Medical University, The Heilongjiang key Laboratory of Anesthesia and Intensive Care Research, Harbin Medical University, Health Road, Nangang District, Harbin, Heilongjiang, People's Republic of China, Email qwj0915@163.com; Meilin Weng, Department of Anesthesiology, Zhongshan Hospital, Fudan University, Shanghai, People's Republic of China, Email weng.meilin1@zs-hospital.sh.cn

Background: Early vascular regeneration is important for the speedy recovery of neurological function following ischemic stroke. M2-like microglia polarization decreases and vascular regeneration weakens with aging. The function of mitochondrial respiratory chain is dependent on M2-like polarization in microglia. *DARS2* gene is a marker for mitochondrial respiratory chain function, but its specific molecular mechanism affecting acute angiogenesis of microglia during ischemic stroke in elderly individuals remains unclear.

Methods: A murine model of middle cerebral artery occlusion (MCAO) was used to perform animal behavioral assessments, immunoblotting, tube formation and chick embryo chorioallantoic membrane assays. A D-galactose-induced cellular senescence model was established in BV2 cells.

Results: Aging significantly exacerbates acute brain injury 24 hours post-cerebral ischemia-reperfusion, with increased expression of M1-like microglial markers and a concomitant decrease in M2-like microglial markers. Additionally, aging can inhibit DARS2 protein expression, adversely affect angiogenesis and reduce brain-derived neurotrophic factor (BDNF) and vascular endothelial growth factor A (VEGFA) expression. In vitro, oxygen-glucose deprivation/reoxygenation and re-glucose (OGD/R) demonstrated that *DARS2* gene knockout in young microglia replicates the phenotypic characteristics observed in aged microglia.

Conclusion: This study suggests that aging impedes M2-like microglial polarization by downregulating DARS2 expression in microglia, thereby impairing emergency angiogenesis during acute ischemic stroke and exacerbating neuronal damage.

Keywords: ischemic stroke, angiogenesis, DARS2, microglia

Background

Ischemic stroke is a notable cause of death and long-term disability in adults worldwide.[1] Aging is an independent risk factor for ischemic stroke. Between 75% and 89% of patients with ischemic stroke are aged 65 years or above, who are more susceptible to complications associated with nerve damage.[2] Age-related changes in immune function can exacerbate brain damage in senescent mice following MCAO.[3] However, the precise mechanisms by which aging potentiates ischemic brain injury remain unclear.

Microglia are innate immune cells in the brain that possess exceptional specialized plasticity, enabling them to adapt to diverse local microenvironments.[4,5] Under physiological conditions, microglia maintain a quiescent state. However, in response to pathological conditions such as tissue damage, inflammation, ischemia, and hypoxia, they are activated and can polarize into two distinct states: M1-like, which facilitates inflammatory responses, and M2-like, which mitigates

https://doi.org/10.2147/JIR.S527147
Received: 31 March 2025
Accepted: 9 September 2025
Published: 8 January 2026

them.[6,7] Importantly, microglia in these polarized states can transition between M1-like and M2-like phenotypes.[8] During acute ischemic brain injury, microglia orchestrate immune responses in the brain.[9] Compared to young mice, the anti-inflammatory/pro-inflammatory ratio of microglia in aged mice is diminished following ischemic stroke,[10,11] suggesting that the modulation of microglial phenotype may be a key mechanism through which aging exacerbates ischemic brain injury.[12,13] However, the underlying molecular mechanisms remain unclear.

Mitochondria are central regulators of microglial metabolism, whose dynamic balance and functional impairments serve as hallmarks of aging.[14] Mitochondria modify the metabolic patterns of sugars, fats, and amino acids in macrophages and modulate their polarization by generating reactive oxygen species (ROS), thereby influencing the outcome of ischemia-reperfusion injury.[15] The mitochondrial respiratory chain is a pivotal regulator of mitochondrial metabolism and exhibits extreme sensitivity to hypoxia. Its activation serves as a physiological marker for macrophage activation and is governed by the *DARS2* gene.[16] We hypothesize that aging may regulate the polarization of microglia after ischemic stroke by affecting mitochondrial respiratory chain function. Research indicates that the early activation of M2-like microglia is vital for nerve regeneration, acute angiogenesis, and synaptic remodeling, which potentially improves the prognosis of ischemic stroke.[17]

This study examined the mechanisms by which aging inhibits M2-like microglial polarization by downregulating DARS2 expression in microglia, consequently suppressing emergency angiogenesis post-ischemic stroke and exacerbating neurological damage.

Methods

Establishment of a Transient Middle Cerebral Artery Occlusion (tMCAO) Model in Old Mice

Two-month-old and Eighteen-month-old male C57BL/6 mice were procured from the China National Laboratory Animal Resource Center (Shanghai). The mice were housed in our animal facilities under controlled conditions (illumination with 200 lux strip lights at cage level; temperature maintained at 22 ± 1°C; and a 12-hour light/dark cycle), with free access to water and food.

tMCAO was induced in the mice using the intravascular suturing technique. The mice were anesthetized with sevoflurane, and a heating system was used to maintain their rectal temperature at 37 ± 0.5°C. tMCAO was achieved by inserting a monofilament nylon suture (catalog number: 602256PK5Re or 602356PK5Re, Doccol, Sharon, USA) through the external carotid artery and advancing it to the left internal carotid artery until minor resistance was encountered. Regional cerebral blood flow (rCBF) was continuously monitored using laser Doppler flowmetry (PeriFlux 5000) during tMCAO in mice. Hemodynamic changes were recorded at baseline (pre-ischemia) and during occlusion, with real-time data analysis performed using the manufacturer's software. A significant decrease of more than 70% in the regional cerebral blood flow (rCBF) from the baseline in the left middle cerebral artery, was used as an indicator of successful cerebral ischemia induction. The mice were re-anesthetized with sevoflurane, and the sutures were removed 90 minutes post-tMCAO. Mice were sacrificed 24 hours after tMCAO, and brain tissues were collected. The hippocampal region and ischemic penumbra were isolated for subsequent analyses. The remaining tissues were uniformly collected and processed by the animal center.

TTC Staining for Cerebral Infarct Assessment

After 24 hours post-tMCAO surgery, the animals were euthanized, and the whole brain tissue was quickly removed. The brains were briefly pre-cooled at −20°C and then coronally sectioned into 2 mm thick slices. The brain slices were immersed in 1% TTC staining solution and incubated at 37°C in the dark for 15–30 minutes. The infarcted area remained pale due to the loss of enzyme activity. After staining, the slices were fixed with 4% paraformaldehyde. Images were captured using a digital camera, and the infarct volume was quantitatively analyzed using ImageJ software. The entire procedure was performed under light-protected conditions, and a sham-operated group was set as the negative control.

Neurological Function Assessment

The neurological functions of the mice were assessed by an investigator, blinded to the experimental procedures, using the Longa score at 24 hours after reperfusion. The grading was based on a 5-point scale: grade 0, no neurological defect; grade 1, failure to extend the affected lateral forepaw, revealing a mild neurological deficit; grade 2, turning to the paralyzed side while walking, demonstrating a moderate neurological deficit; grade 3, vulnerable to falling on the paralyzed side, indicating a severe neurological deficit; and grade 4, inability to walk voluntarily and unconsciousness. A neurological deficit score of 1–3 was considered a successful model.

Cell Culture

The cells were cultured and maintained at 37°C with 5% CO_2. Mouse microglia BV2 cells (catalog number: CL-0493A, Pricella, Wuhan, China) were cultured in MEM supplemented with 10% fetal bovine serum (FBS) and 1% penicillin/streptomycin. The aging microglia model was established by stimulating BV2 cells with different concentrations of D-galactose. Aging microglia were cultured with 50 nM D-galactose for 3 days, and the degree of aging was identified using β-galactosidase staining. Mouse brain microvascular endothelial cells (MBMEC) (catalog number: CP-M108, Pricella, Wuhan, China) were cultured in Dulbecco's Modified Eagle Medium (DMEM) supplemented with 10% FBS and 1% penicillin/streptomycin.

Cell Viability Assay

The effect of D-galactose on cell viability was detected using the cell counting kit-8 (CCK-8) assay (catalog number: K1018, APExBIO). BV2 cells were seeded in 96-well plates at 1×10^3 cells/well and cultured at 37°C for 3 days. Thereafter, the cells were treated with D-galactose (0, 20, 50, 100 μM) for 3 days. Subsequently, 10 μL CCK-8 solution was added to each well, and the incubation was continued for 2 hours at 37°C. Absorbance at 450 nm was measured using a microplate reader (Bio-Rad).

Enzyme-Linked Immunosorbent Assay (ELISA)

ELISA kits were used to detect the concentrations of interleukin-10 (IL-10) (catalog number: JM-02459M1, JINGMEI BIOTECHNOLOGY, JiangSu, China), cytokine tumor necrosis factor-alpha (TNF-α) (catalog number: ZC-39024, ZCIBIO, Shanghai, China), interleukin-1β (IL-1β) (catalog number: ZC-37974, ZCIBIO, Shanghai, China) and interleukin-6 (IL-6) (catalog number: ZC-37988, ZCIBIO, Shanghai, China) in the brain. The brain tissues were homogenized on ice in RIPA buffer (catalog number: P0013B, Beyotime, Shanghai, China) composed of 25 mM Tris-HCl, pH 7.6, 150 mM NaCl, 1% sodium deoxycholate, 0.1% SDS and a protease inhibitor cocktail containing 10 mg/mL aprotinin, 5 mg/mL pepstatin, 5 mg/mL leupeptin and 1 mM phenylmethanesulfonyl fluoride (PMSF). The supernatant was collected after centrifuging at 13,000 × g for 20 minutes at 4°C, and the protein concentration was measured with the bicinchoninic acid (BCA) assay. Briefly, a standard curve was generated using bovine serum albumin ranging from 0 to 2 mg/mL. Test samples from the ischemic penumbra brain tissue were appropriately diluted in PBS, and 25 μL of each standard or sample was mixed with 200 μL of BCA working reagent (50:1 mixture of reagents A and B) in a 96-well plate. After incubation at 37°C for 30 min, the absorbance was measured at 562 nm using a microplate reader. The protein concentration of ischemic penumbra tissue samples was calculated by comparing their absorbance values to the standard curve. Cytokine concentrations were then determined after normalization to the total protein content. ELISA was performed conforming to the manufacturer's instructions of the respective kits.

Chick Embryo Chorioallantoic Membrane Assay

Fertilized specific pathogen-free (SPF) eggs were procured from the Beijing Merial Vital Laboratory Animal Technology. The eggs were placed in a hatching incubator maintained at 37.5°C with 60–70% relative humidity, and were rotated every 5 minutes. All SPF chick embryos utilized in this study were evaluated from 18 hours post-fertilization to embryonic day 15. A volume of 50 μL of serum and cell supernatant from each group mouse was injected into the

blood vessels of the chicken embryos. Photographs were taken at 20, 40, 60, 120 and 180 minutes post-injection to analyze the vascular area at each time point. The ImageJ software was used for analyses of all images.

Oxygen-Glucose Deprivation (OGD)

BV2 cells underwent OGD after reaching 80−90% confluence. Briefly, BV2 cells were incubated in a glucose-free balanced salt solution (BSS) and placed in a hypoxic incubator maintained at 0.2% O_2, 5% CO_2, and 70% humidity for 1 hour (Toepffer Lab Systems, Goeppingen, Germany). For the reoxygenation and re-glucose phase, the BSS was replaced with standard cell culture medium, and the cells were incubated at 37°C in a 5% CO_2 incubator for 24 hours. Subsequently, the cells were prepared for further experimental procedures.

Transfection of Microglia with DARS2 Small Interfering RNA (siRNA)

BV2 cells were transiently transfected with siRNA targeting mouse DARS2 (catalog number: abx913574, Abbexa, UK) or a negative control siRNA using Lipofectamine 2000 transfection reagent in a serum-free medium, as per the manufacturer's instructions. The most effective siRNA sequence was selected from those provided by Qiagen. The efficacy of all siRNAs was evaluated through mRNA knockdown analysis via Western blotting. After incubating the cells for 24 hours post-transfection, they were used for subsequent experiments.

Flow Cytometry

The accumulation of reactive oxygen species (ROS) in microglia was quantified using a ROS assay kit (catalog number: S0033S, Beyotime, Shanghai, China) with 2′, 7′-dichlorofluorescin diacetate (DCFH-DA) as the fluorescent probe. The non-fluorescent DCFH-DA permeates the cell membrane and is hydrolyzed by intracellular esterases to DCFH, which is then oxidized by intracellular ROS to produce fluorescent DCF. The cells in each experimental group were subjected to the aforementioned treatment protocol. Following digestion and collection by trypsin, the cells were suspended at a concentration of 5×10^6 cells/well in a centrifuge tube containing 10 μmol DCFH-DA. The suspension was then incubated at 37°C for 30 minutes, with periodic inversion every 3–5 minutes. The cells were washed three times with serum-free medium and resuspended in 400 μL of cold phosphate-buffered saline (PBS). ROS levels in microglia were immediately assessed using flow cytometry.

Western Blotting

The cells were collected and washed with PBS. Protein samples from all experimental conditions were obtained through cell lysis for 30 minutes using RIPA buffer (catalog number: P0013B, Beyotime, Shanghai, China) supplemented with the protease inhibitor PMSF (catalog number: P1005, Beyotime, Shanghai, China). Following centrifugation to remove cell debris, the protein concentrations were determined. The proteins were then separated on a 10% sodium dodecyl sulphate-polyacrylamide gel electrophoresis (SDS-PAGE) gel (catalog number: P0690, Beyotime, Shanghai, China) and transferred to a polyvinylidene fluoride (PVDF) membrane (catalog number: 63116500, Roche, UK). The PVDF membrane was blocked with 5% skimmed milk for 2 hours, followed by incubation with primary antibodies to anti-inducible nitric oxide synthase (iNOS) (1:2000; catalog number: A3774, Abclonal, Wuhan, China), anti-triggering receptor expressed on myeloid cells 2 (TREM2) (1:2000; catalog number: A23432, Abclonal, Wuhan, China), anti-DARS2 (1:2000; catalog number: A7813, Abclonal, Wuhan, China), anti-P53 (1:50000; catalog number: 10442-1-AP, Proteintech, USA), anti-Arg1 (1:1000; catalog number: WL02825, Wanleibio, China), anti-VEGFA (1:1000; catalog number: 12303, Abclonal, Wuhan, China), anti-BDNF (1:1000; catalog number: ab203573, Abcam, USA) for 14 hours at 4°C. The blots were incubated with a goat anti-rabbit secondary antibody coupled with horseradish peroxidase for 50 minutes at room temperature. The enhanced chemiluminescence kit (catalog number: P0018S, Beyotime, Shanghai, China) was used for detection. The chemiluminescence results were recorded with an imaging system (Bio-Rad).

Tube Formation Assay

To investigate the angiogenic potential of BV2 cells in vitro, a matrix gel tube formation assay was conducted. MBMEC were cultured until the third to fourth passage and subsequently divided into three groups: control,

young, and old. A six-well plate was coated with Matrigel substrate (diluted 1:1 in the base ECM; 500 μL mixture/well) (catalog number: 354234, Corning, USA) and incubated at 37°C for 30 minutes to ensure gel solidification. MBMEC were plated at a density of 2×10^6 cells/well and cultured with supernatants collected from the control, young, and old microglial cells post-OGD/R. The cells were incubated at 37°C with 5% CO_2 for 6 hours to promote tubular network formation. These networks were observed and imaged using an inverted microscope (DMi8, Zeiss, Germany), followed by analysis with ImageJ software (Rawak Software Inc, Stuttgart, Germany).

Immunohistochemistry

Briefly, the mouse brain was fixed in 4% paraformaldehyde at 4°C for 24 hours, and then dehydrated and embedded in paraffin. Thereafter, 5-μm coronal sections of the cerebral hemisphere were cut sequentially and mounted on slides. The paraffin sections were baked, deparaffinized, hydrated and washed before blocking with 10% donkey serum (catalog number: SL050, Solarbio, Beijing, China) or goat serum (catalog number: SL038, Solarbio, Beijing, China). The sections were incubated with a primary antibody to anti-vascular endothelial growth factor A (VEGFA) (catalog number: A17877, Abcolonal, Wuhan, China) overnight. After reheating for 1 hour, the sections were incubated with a secondary antibody for 1 hour, followed by 3, 3′-diaminobenzidine (DAB) staining, hematoxylin counterstaining, dehydration and sealing.

Statistical Analysis and Reproducibility

GraphPad Prism 9.5.1 software was used for statistical analysis in this study. The data are presented as mean ± standard deviation (SD). Small samples tend to conform to a normal distribution. The normality of the data was examined using the Shapiro–Wilk test. The homogeneity of variance was assessed by the Brown-Forsythe test (≥3 groups). The analysis of variance (ANOVA) was used when the assumptions (equal variance and normal distribution) were met, otherwise non-parametric tests were used to analyze the differences, and multiple comparisons were performed using the Tukey or Dunn's test.

Results

Aging Suppresses Angiogenesis During Acute Ischemic Stroke and Aggravates Ischemic Brain Injury

To examine the effects of aging on neurological function impairment and neuroinflammation in mice post-ischemic stroke, we performed an in vivo experiment, as illustrated in Figure 1A. There was no significant difference in the percentage of blood flow reduction between the two groups of mice following 90 minutes of MCAO (Figure 1B). However, the old mice showed a significantly larger infarct volume, higher neurological deficit scores, poorer performance on the rotarod test, shorter total movement distance, slower average movement speed, and longer total resting time at 24 hours post-MCAO, compared to the young group (Figure 1C–F). Furthermore, the expression of brain-derived neurotrophic factor (BDNF), a key neuroprotective factor, was markedly downregulated in the ischemic penumbra (IP) and hippocampus (Hipp) in the old group (Figure 1G and H). These findings indicate that aging exacerbates neurological and motor function impairments following ischemic stroke.

Compared to the young group, the old group demonstrated a downregulation of Zonula occludens 1 (ZO1), occludin, and VEGFA expression in the frontal cortex, which are associated with angiogenesis, as well as a downregulation of VEGFA expression in the hippocampus at 24 hours post-MCAO (Figure 1G–I). To further substantiate the relationship between aging and angiogenesis, a chick embryo chorioallantoic membrane assay was used, which showed a reduced capacity of the sera from the old group to stimulate angiogenesis compared to the young group (Figure 2A). Immunohistochemical assays further confirmed a significant downregulation of VEGFA expression in the ischemic penumbra of the old group (Figure 2B). Collectively, these findings suggest a substantial decline in the angiogenic potential of aged mice after cerebral ischemia-reperfusion.

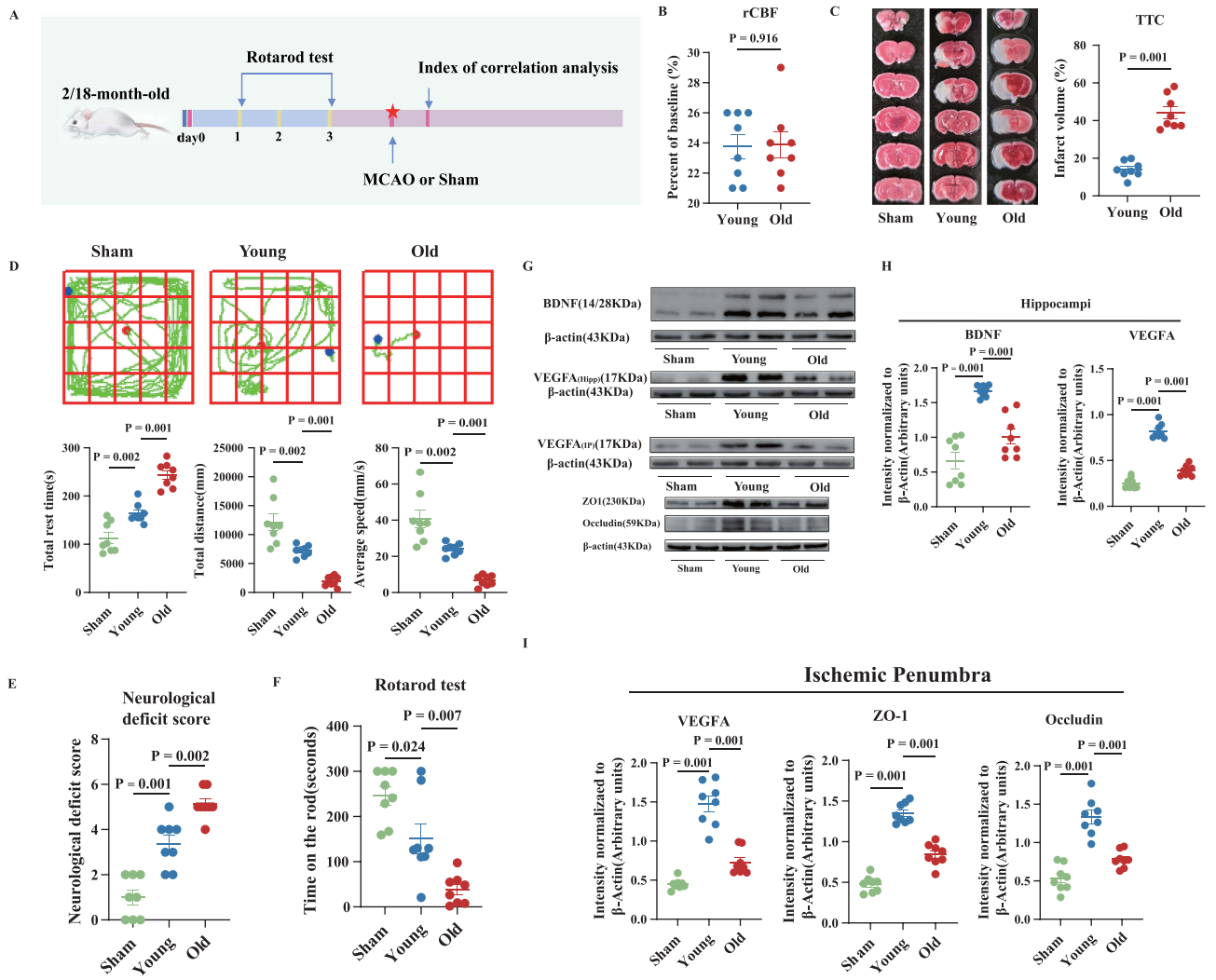

Figure 1 During acute ischemic stroke in old mice, neurological damage worsens, with a concomitant decrease in the expression of markers and proteins involved in angiogenesis. (**A**) Experimental design. (**B**) Percentage of cerebral blood flow relative to the baseline in the young (Two-month-old) and old (Eighteen-month-old) groups after MCAO. (**C**) Representative brain slice images stained with 2,3,5-triphenyltetrachlorozole (TTC) and statistical graphs. (**D–F**) Representative performance in the 24-hour open field test, neurological deficit score, and the rotarod test after MCAO. (**G–I**) The relative levels and corresponding quantitative data of BDNF and VEGFA, as well as ZO1, and occludin proteins in the ischemic penumbra of mouse hippocampus 24 hours after MCAO. Normally distributed parametric data are shown as mean ± standard error of the mean (SEM) (**B–F**), (**H–I**). Data of each animal is also presented n = 8 for (**B–F**), (**H–I**). Normality was confirmed using Shapiro–Wilk tests (all p>0.05), permitting the use of parametric independent two-sample t-tests.

Aging Suppresses Angiogenesis by Inhibiting the M2-Like Polarization of Microglia

Compared to the young group, the old group exhibited upregulated iNOS expression and downregulated TREM2 and Arg1 expression (Figure 2C–J). Furthermore, 24 hours post-MCAO, the old group demonstrated a notable elevation in IL-1β and IL-6, accompanied by a significant reduction in IL-4 and IL-10 in ischemic penumbra (Figure 2K–N). These findings indicate that aging disrupts the microglial polarization balance between the proinflammatory M1-like phenotype and the anti-inflammatory M2-like phenotype, thereby intensifying the acute neuroinflammatory response following ischemic stroke and exacerbating early neurological impairment. Given that IL-4 promotes emergency angiogenesis in the brain post-ischemic stroke,[18] the results suggest that aging-induced inhibition of microglial M2-like polarization may further exacerbate neuronal damage by suppressing this critical regenerative process.

To further substantiate the aforementioned hypothesis, we conducted in vitro experiments (Figure 3A) involving β-galactosidase staining, the CCK-8 assay, evaluated the aging protein P53, and measured ROS via flow cytometry to demonstrate that 50 mM D-galactose can induce aging in microglia while concurrently reducing cell death (Figure 3B–F). The old group received 50 mM D-galactose in the culture medium, whereas the young group received an equal volume of

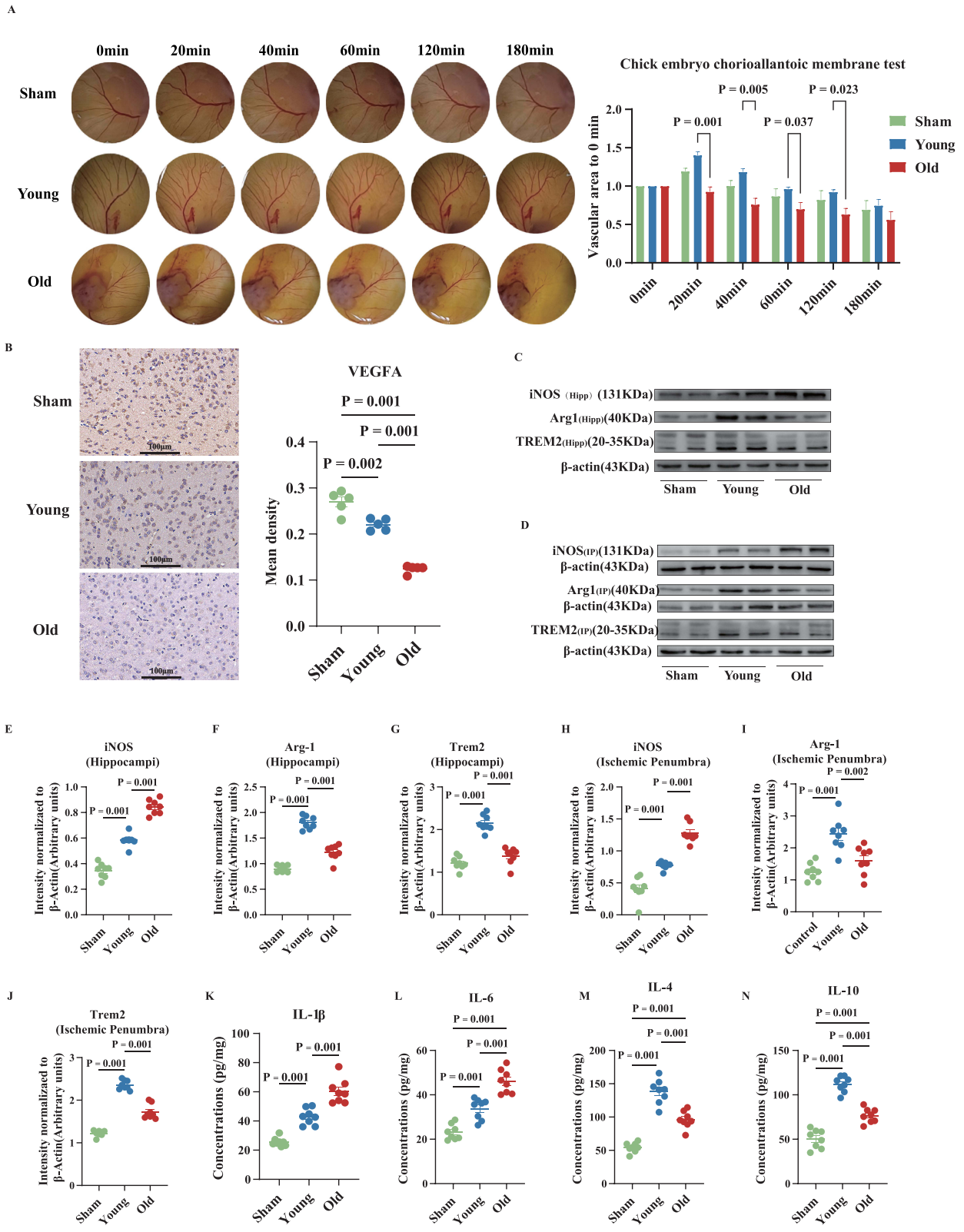

Figure 2 During acute ischemic stroke in old mice, compensatory neovascularization markers are reduced, serum stimulation of angiogenesis is weakened, and polarization of M1-like microglia is increased. (**A**) The ability of peripheral blood to stimulate angiogenesis in mice after 24 hours of MCAO was detected using the chick embryo chorioallantoic membrane assay. (**B**) Immunohistochemical detection of relative expression and quantitative data of VEGFA in the brain after 24 hours of MCAO in mice. (**C–J**) The relative levels and corresponding quantitative data of iNOS, Arginase 1 (Arg1), and TREM2 proteins in the hippocampus and left frontal cortex (FrA) of mice 24 hours after MCAO. (**K–N**) IL-1β, IL-6, IL-4, and IL-10 levels in the left FrA of the brain were detected by ELISA 24 hours after MCAO. Normally distributed parametric data are shown as mean ± SEM (**A** and **B**), (**E–N**). Data of each animal is also presented n=3 for (**A**) n=5 for (**B**) n=8 for (**J–N**). Normality was confirmed using Shapiro–Wilk tests (all p>0.05), permitting the use of parametric independent two-sample t-tests.

https://doi.org/10.2147/JIR.S527147

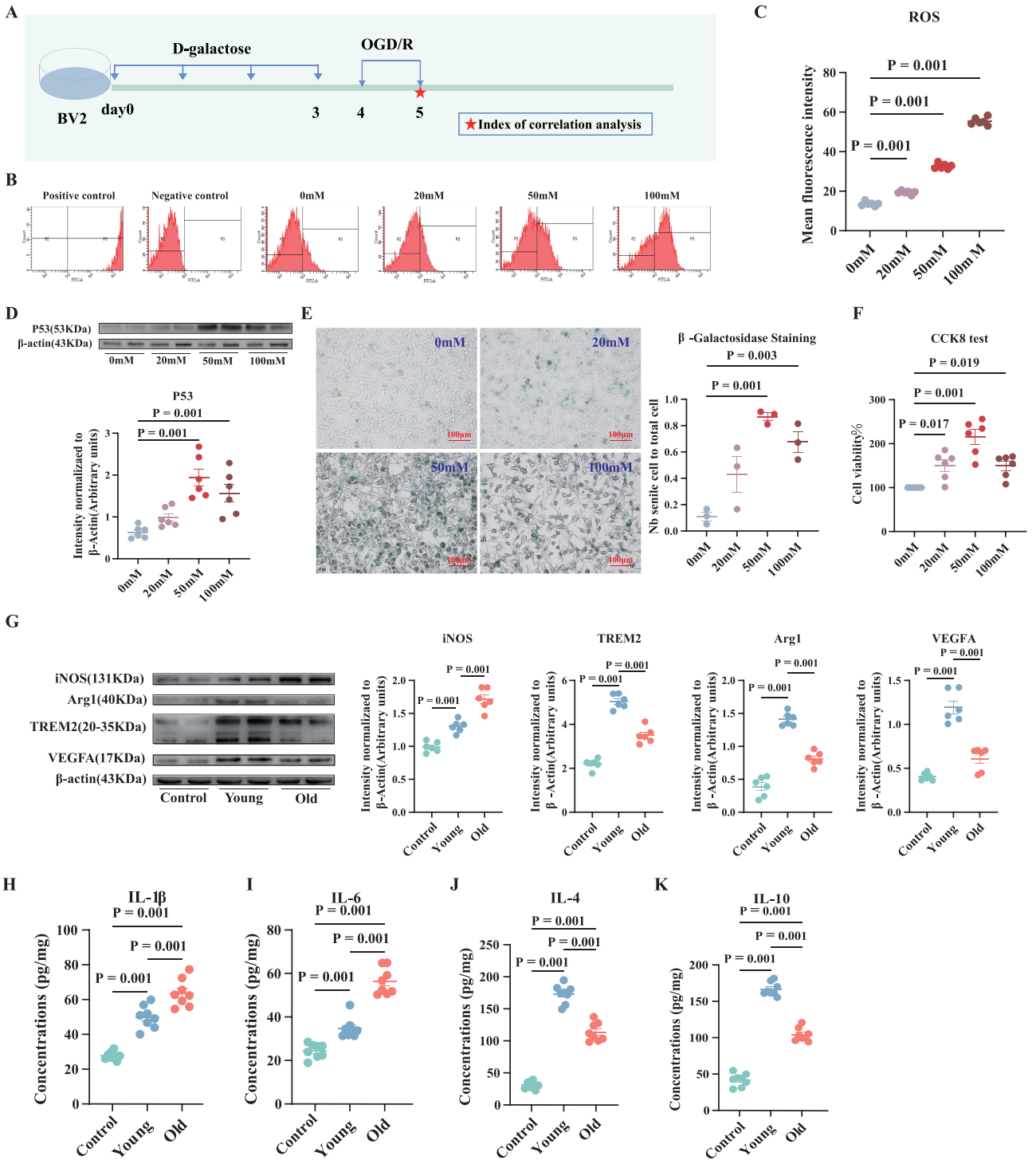

Figure 3 D-galactose-induced aging microglia exhibit reduced polarization towards M2 after OGD/R, which decreases their ability to stimulate angiogenesis. (**A**) Experimental design. (**B–F**) The relevant results of different concentrations of D-galactose-induced P53 expression in microglia, supernatant ROS, β-galactose staining, and CCK-8 assay. (**G**) The relative levels and corresponding quantitative data of iNOS, Arg1, TREM2, and VEGFA proteins 24 hours after OGD/R. (**H–K**) IL-1β, IL-6, IL-4, and IL-10 levels in the microglial cell supernatants were detected by ELISA 24 hours after OGD/R. Normally distributed parametric data are shown as mean ± SEM (**B**), (**D–K**). Data of each animal is exhibited n = 5 for (**C**), n = 6 for (**D** and **F–G**), n = 3 for (**E**), n = 8 for (**G–K**). Normality was confirmed using Shapiro–Wilk tests (all p>0.05), permitting the use of parametric independent two-sample t-tests.

untreated medium. After one hour of OGD, followed by 24 hours of reoxygenation and re-glucose, we assessed the expression levels of proteins associated with microglial polarization. The findings revealed upregulated iNOS expression and downregulated TREM2 and Arg1 expression in the old group as compared to the young group (Figure 3G).

https://doi.org/10.2147/JIR.S527147

Furthermore, the old group demonstrated a marked elevation in IL-1β and IL-6 levels in the cell supernatant, while IL-4 and IL-10 levels were significantly reduced compared to the young group (Figure 3H–K). Additionally, VEGFA expression was significantly decreased in the old group compared to the young group (Figure 3G). The microglial cell culture medium supernatant was used for the tube formation and chick embryo chorioallantoic membrane assays. The findings revealed a significant decrease in the number of nodes, tubules, and branches, as well as reduced angiogenesis in the old group compared to the young group (Figure 4A and B). Furthermore, the old group demonstrated lower mitochondrial membrane potential as compared to the young group (Figure 4C).

These findings imply that aging may enhance inflammatory responses and inhibit angiogenesis by preventing the polarization of M2-like microglia after OGD, potentially due to mitochondrial damage in the microglia.

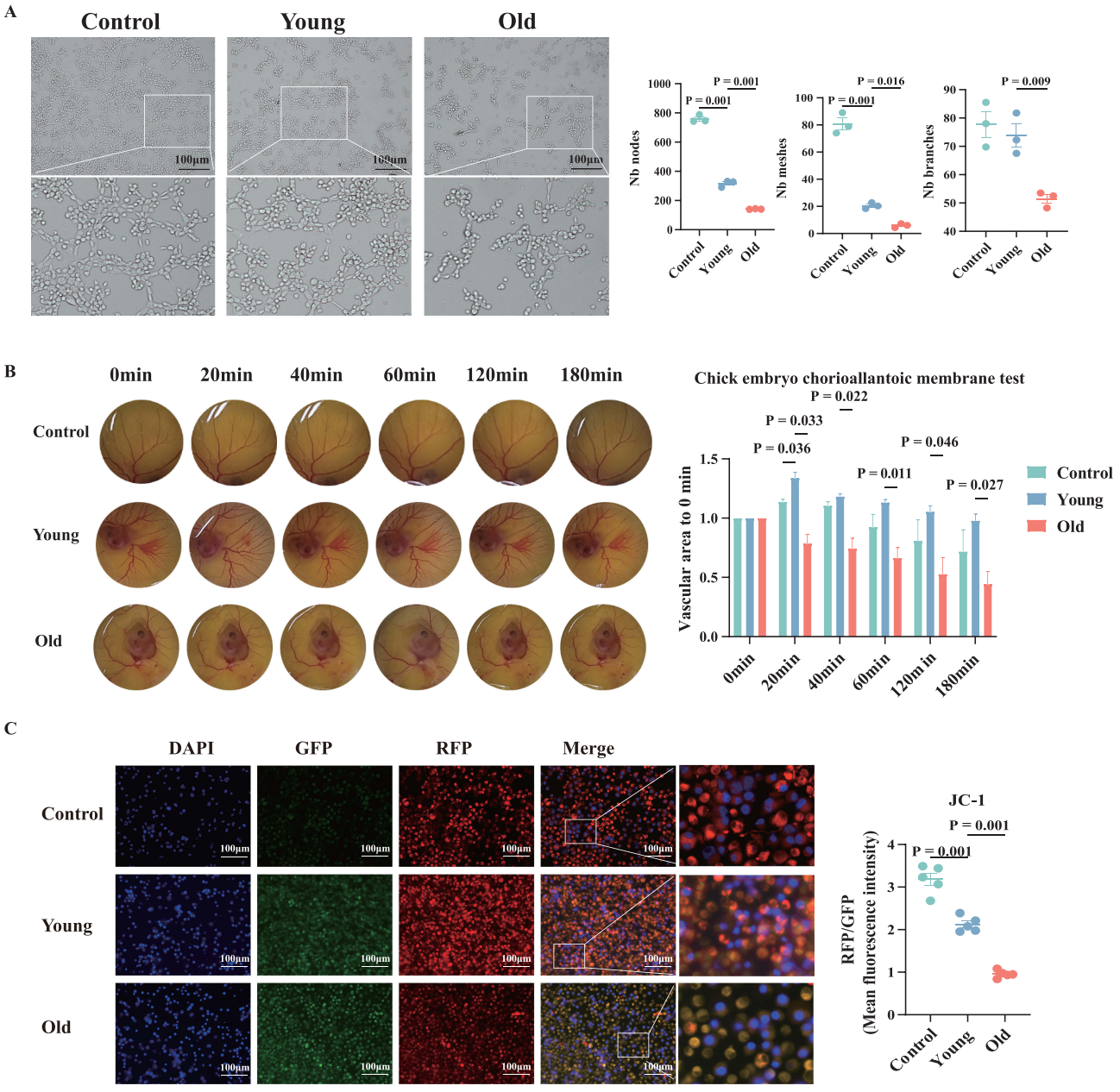

Figure 4 D-galactose-induced aging microglia exhibit reduced polarization towards M2 after OGD/R, which decreases their ability to stimulate angiogenesis. (**A** and **B**) The ability of different groups of microglial cell supernatants to stimulate angiogenesis was tested using the matrix gel tube and chick embryo chorioallantoic membrane assays. (**C**) JC-1 staining and statistical graph of microglia after OGD/R. Normally distributed parametric data are shown as mean ± SEM (**A**–**C**). Data of each animal is shown n = 3 for (**A**), n = 3 for (**B**), n = 5 for **(C)**. Normality was confirmed using Shapiro–Wilk tests (all p>0.05), permitting the use of parametric independent two-sample t-tests.

https://doi.org/10.2147/JIR.S527147

Aging Suppresses M2-Like Polarization of Microglia and Ultimately Angiogenesis by Downregulating the Mitochondrial Respiratory Chain-Associated Gene DARS2

To confirm the involvement of microglial mitochondrial damage in the regulation of acute angiogenesis following aging-suppressed ischemic stroke, we analyzed the expression of the mitochondrial respiratory chain-related gene *DARS2* in both in vivo and in vitro models. A significant downregulation of DARS2 expression was observed in the old group (Figure 5A–D). In vitro experiments involving the knockout of DARS2 (Figure 5A, E and F), showed a major reduction in mitochondrial membrane potential in the si-young group compared to the young group (Figure 5K).

Additionally, immunoblotting, tube formation and chick embryo chorioallantoic membrane assays indicated a notable decrease in the number of nodes, tubules, and branches, as well as reduced angiogenesis in the si-young group

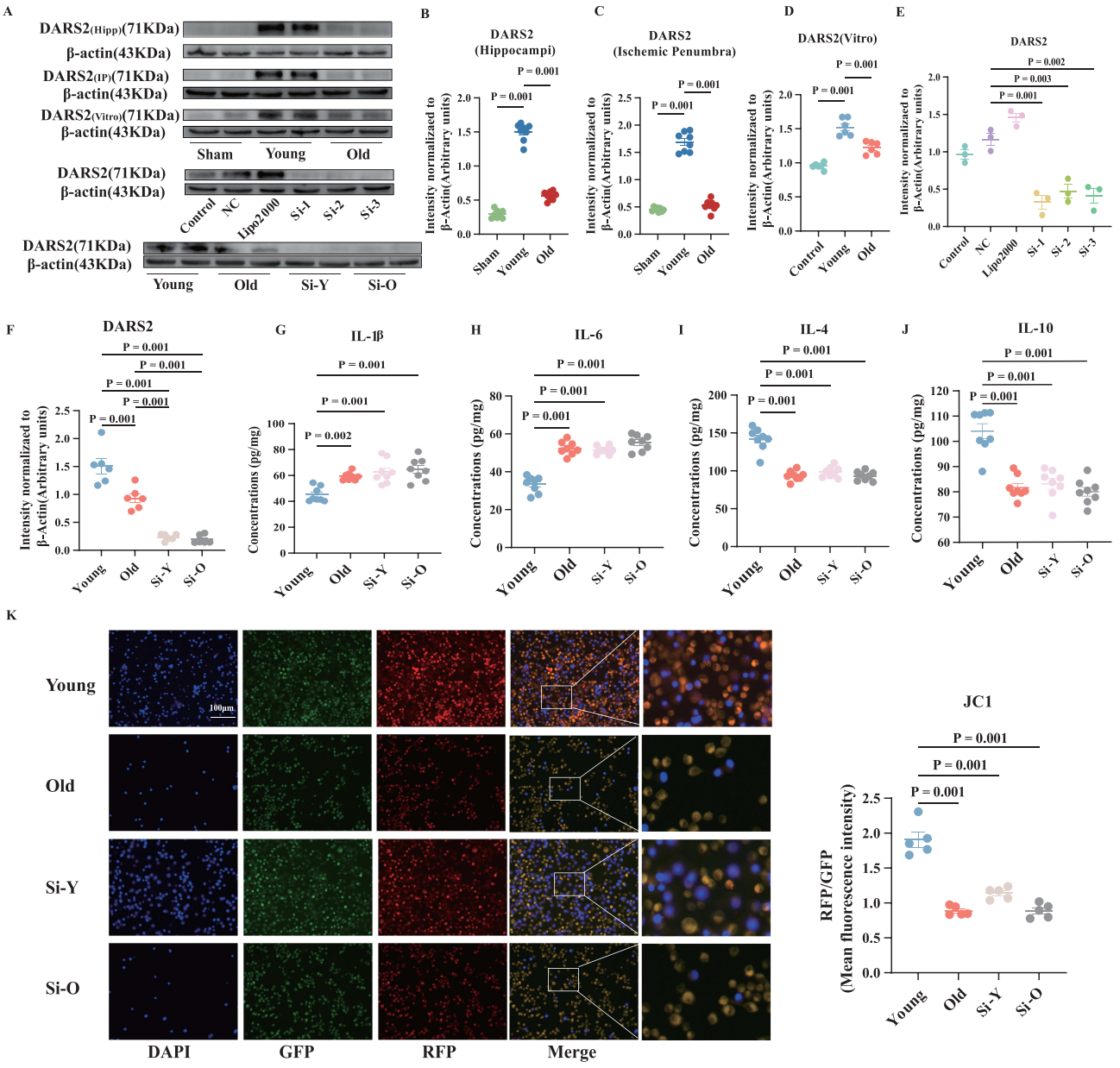

Figure 5 Aging downregulates the mitochondrial respiratory chain related gene *DARS2*, inhibits polarization of microglia M2-like, and suppresses angiogenesis. (**A–F**) The relative levels and corresponding quantitative data of DARS2 protein in animal experiments, cell experiments, and cell knockout experiments. (**G–J**) After knocking out DARS2, the concentration of IL-1β, IL-6, IL-4, and IL-10 in the supernatant of microglial cells was detected by ELISA 24 hours after OGD/R. (**K**) JC-1 staining and statistical plots of microglia after OGD/R. Normally distributed parametric data are shown as mean ± SEM (**B–K**). Data of each animal is presented n = 8 for (**B** and **C**) and (**G–J**), n = 6 for (**D** and **F**) n = 3 for (**E**), n = 5 for (**K**). Normality was confirmed using Shapiro–Wilk tests (all p>0.05), permitting the use of parametric independent two-sample t-tests.

https://doi.org/10.2147/JIR.S527147

(Figure 6A and B). Compared to the young group, the si-young group showed increased iNOS expression and significant downregulation of TREM2, Arg1, and VEGFA expression (Figure 6C). Notably, the expression of anti-inflammatory IL-4 and IL-10 was decreased, along with an increase in the expression of pro-inflammatory IL-1β and IL-6 (Figure 5G–J). These results suggest that DARS2 promotes M2-like polarization and inhibits M1-like polarization of microglia following OGD/R, thereby mitigating inflammatory responses and enhancing the angiogenic function of microglia.

Discussion

This study presents a novel perspective on the therapeutic potential of microglial polarization in mitigating acute neurological deficits following ischemic stroke in aged mice. Aging was found to exacerbate brain function impairment following ischemic stroke by downregulating the *DARS2* gene in microglia, thereby suppressing the polarization of M2-like microglia and inhibiting angiogenesis (Figure 7). These findings suggest that the disruption of polarization homeostasis of microglia during aging contributes to the age-related decline in angiogenesis and brain repair processes post-stroke.

Aging is a primary risk factor for ischemic stroke.[19] Over the past three decades, major advancements in the prevention and treatment of ischemic stroke have resulted in a marked reduction in stroke incidence among individuals under 60 years of age. However, the outcomes for ischemic stroke patients aged 60–80 years remain suboptimal. This

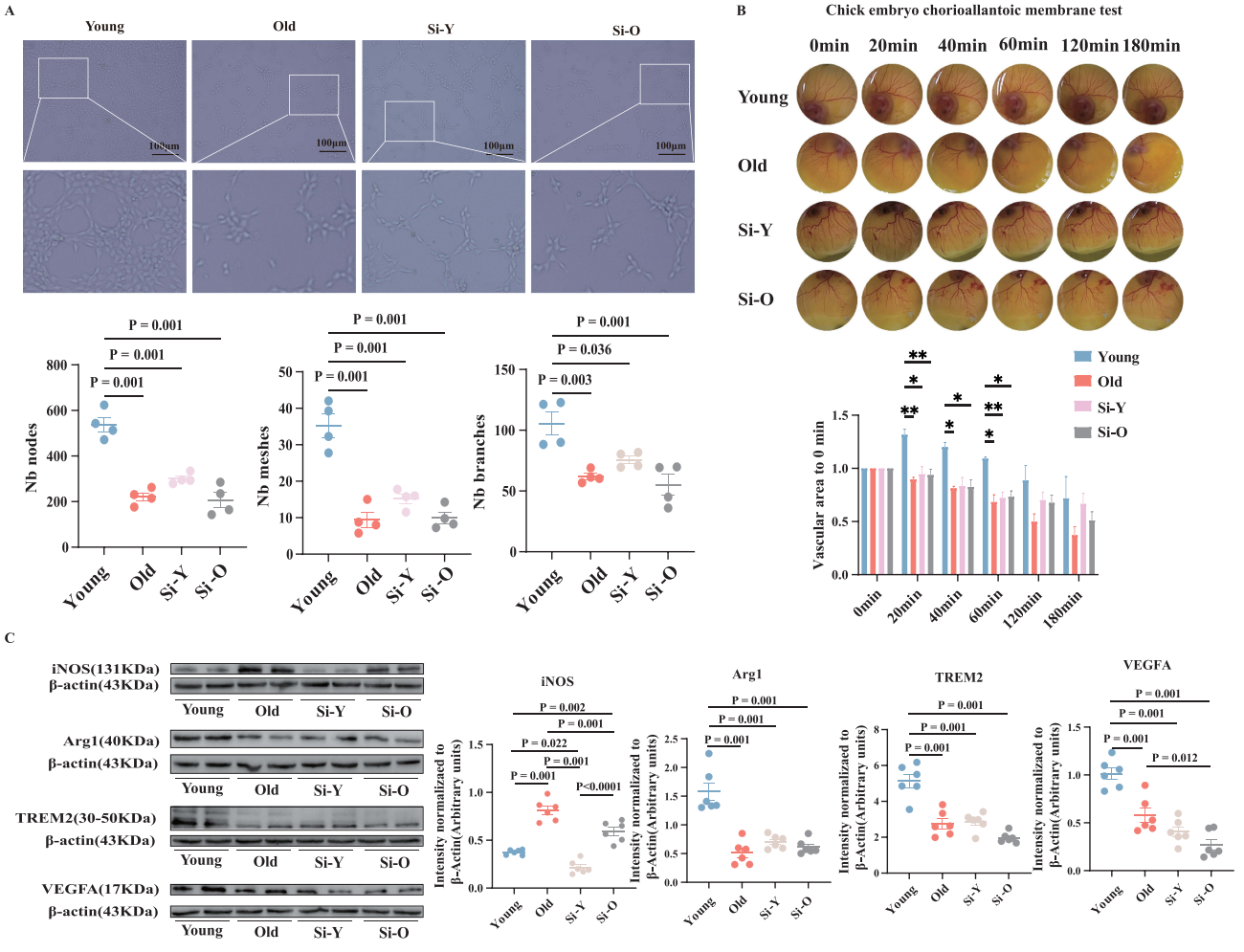

Figure 6 (**A** and **B**) The ability of different groups of microglial cell supernatants to stimulate angiogenesis was tested using the matrix gel tube and chick embryo chorioallantoic membrane assays. (**C**) Relative levels and corresponding quantitative data of iNOS, Arg1, TREM2, and VEGFA proteins in microglia 24 hours after OGD/R. Normally distributed parametric data are shown as mean ± SEM (**A**–**C**). Data of each animal is displayed n = 4 for (**A**), n = 3 for (**B**), n = 6 for (**C**). Normality was confirmed using Shapiro–Wilk tests (all p>0.05), permitting the use of parametric independent two-sample t-tests. "*" is defined as P < 0.05, "**" is defined as P < 0.01, "***" is defined as P < 0.001.

https://doi.org/10.2147/JIR.S527147

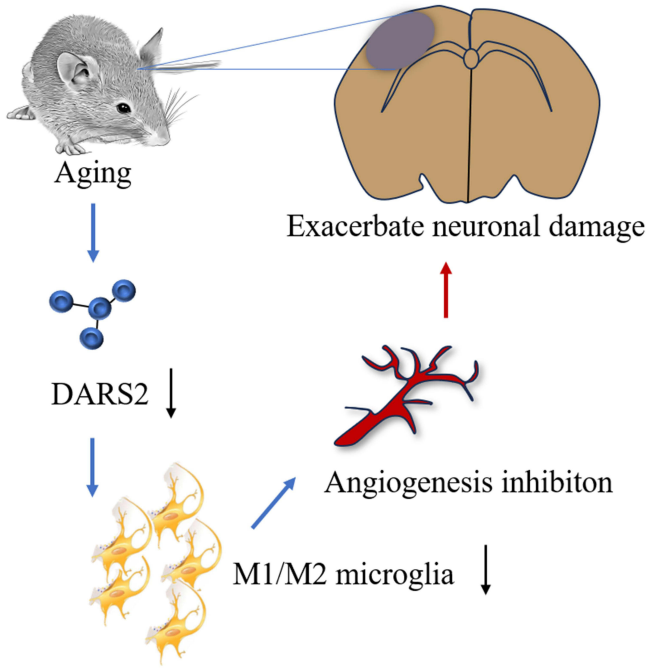

Figure 7 Diagrammatic presentation of the findings from this study. Aging was found to exacerbate brain function impairment following ischemic stroke by downregulating the DARS2 gene in microglia, thereby suppressing the polarization of M2 microglia and inhibiting angiogenesis.

underscores the necessity of prioritizing the elderly population in ongoing efforts for ischemic stroke prevention and management.[20] Current research is focused on the endogenous brain repair processes following ischemic stroke, which include angiogenesis and oligodendrocyte generation.[21] Angiogenesis is a multifaceted physiological process that encompasses the migration, proliferation, and differentiation of endothelial cells, culminating in the formation of new blood vessels. This process promotes long-term functional recovery after ischemic stroke in aged mice.[22] While cerebral ischemia can induce angiogenesis, aging hinders this process. Previous research indicated that compensatory angiogenesis is attenuated in elderly individuals post-stroke.[23,24] The present study demonstrated more severe neuronal damage following ischemic stroke in older mice compared to young mice. The expression of proteins associated with angiogenesis, including VEGFA, ZO1, and occludin, was notably downregulated within the ischemic penumbra of brain tissue in aged mice. These findings indicate that the acute angiogenic response in the ischemic region of brain tissue is diminished in aged mice following ischemic brain injury, potentially exacerbating the severity of the injury.

There is a negative correlation between angiogenesis and the degree of inflammation post-stroke.[25] Microglia are pivotal cells within the brain that modulate inflammatory responses. Empirical evidence indicates that microglia significantly contribute to angiogenesis post-stroke. Single-cell sequencing of microglia from both aged and young mice, conducted 14 days post-middle cerebral artery occlusion (MCAO), demonstrated that the upregulation of genes promoting angiogenesis in microglia from aged mice was inhibited, correlating with a reduction in neovascularization.[26] Aging can hinder brain function recovery by decreasing signal transmission between microglia and other cells following MCAO, as well as by downregulating the genes associated with angiogenesis.[27] In the present study, aged mice exhibited higher inducible nitric oxide synthase (iNOS) expression and lower triggering receptor expressed on myeloid cells 2 (TREM2) and arginase 1 (Arg1) expression in the ischemic penumbra region of the brain 24 hours post-MCAO, in contrast to young mice. This finding suggests a disruption in the polarization homeostasis of microglia, favoring a shift towards M1-like polarization following ischemic stroke in aged mice. Furthermore, the reduction in M2-like polarization is accompanied by increased M1-like polarization in microglia following ischemic brain injury in aged mice. Collectively, these findings strongly suggest that the polarization state of microglia post-cerebral ischemia is a critical factor influencing angiogenesis and a major mechanism underlying the decreased angiogenesis observed in aged mice after ischemic brain injury.

Mitochondria are key players in the metabolic activities of microglia and their homeostatic imbalance and dysfunction serve as indicators of aging.[28] The activation of the mitochondrial respiratory chain, which serves as a physiological marker of macrophage activation,[16] is modulated by the *DARS2* gene. A previous study employing a mouse skin injury model demonstrated that the targeted knockout of the *DARS2* gene, which impairs mitochondrial respiratory chain function, leads to delayed wound healing by inhibiting the angiogenic activity of M1-like macrophages.[29] M2-like microglia play a pivotal role in promoting angiogenesis in the brain. The activation of these cells coincides with angiogenesis around damaged lesions, thereby facilitating tissue reorganization, enhancing functional recovery, and contributing to the rehabilitation process following spinal cord injury.[30] The upregulation of M2-like microglia stimulates the proliferation of microglia, astrocytes, oligodendrocytes, and CD45 cells, thereby promoting the recovery after brain injury.[31] This study has identified a significant downregulation in the expression of the mitochondrial respiratory chain-associated gene *DARS2*, which is instrumental in regulating angiogenesis through the modulation of macrophage polarity. Consequently, we hypothesize that aging may promote M1-like polarization in microglia, concomitantly with the downregulation of *DARS2* gene expression. The *DARS2* gene knockout experiments showed increased M1-like polarization, with concomitantly decreased M2-like polarization in microglia. These findings suggest that DARS2 functions as an upstream regulator of microglial polarization, facilitating the recovery of brain function following ischemic stroke.

Conclusion

This study validates the phenotypic shift of microglia from M2-like to M1-like in aged mice subjected to ischemic stroke, establishing a correlation between these alterations and both angiogenesis and mitochondrial respiratory chain function. The molecular mechanisms by which microglia influence angiogenesis were clarified through experiments involving the modulation of DARS2. Aging was definitively shown to inhibit compensatory angiogenesis and aggravate neuronal injury via DARS2 downregulation. These findings may facilitate the development of innovative strategies in the future aimed at improving the neurological function in elderly stroke patients.

Highlights

- DARS2 participates in polarization of microglia cells.
- Postoperative neurological damage caused by acute angiogenesis inhibition after ischemic stroke in elderly mice.

Abbreviations

MCAO, middle cerebral artery occlusion; BDNF, brain-derived neurotrophic factor; VEGFA, vascular endothelial growth factor A; OGD/R oxygen-glucose deprivation/reoxygenation and re-glucose; ROS, reactive oxygen species; tMCAO, transient middle cerebral artery occlusion; rCBF, regional cerebral blood flow; MBMEC, Mouse brain microvascular endothelial cells.

Data Sharing Statement

The datasets used and/or analysed during the current study are available from the corresponding author on reasonable request.

Ethics Approval and Consent to Participate

All animal experiments were strictly conducted in accordance with the 3R principles (Replacement, Reduction, Refinement) and were approved by the Animal Ethics Committee of the Second Affiliated Hospital of Harbin Medical University (Approval No. SYDW2023-020).

All mice were housed in specific pathogen-free (SPF) conditions, with their health status monitored daily by professional staff. Surgical procedures were performed under sevoflurane anesthesia supplemented with lidocaine analgesia. Strict aseptic techniques were maintained throughout all operations. To minimize suffering, euthanasia was performed by rapid cervical dislocation.

Author Contributions

All authors made a significant contribution to the work reported, whether that is in the conception, study design, execution, acquisition of data, analysis and interpretation, or in all these areas; took part in drafting, revising or critically reviewing the article; gave final approval of the version to be published; have agreed on the journal to which the article has been submitted; and agree to be accountable for all aspects of the work.

Funding

The study was funded by the Program for Young Talents of Basic Research in Universities of Heilongjiang Province (grant number: YQJH2023028), the Natural Science Foundation of Heilongjiang Province, China (grant number: PL2024H104), National Natural Science Foundation of China (No. 82372502), Shanghai 2023 Medical Innovation Research Special Funding (No. 23Y11902300) and Zhongshan Hospital Clinical Research Project (No. ZSLCYJ202348).

Disclosure

The authors declare that they have no competing interests.

References

1. GBD 2021 Stroke Risk Factor Collaborators. Global, regional, and national burden of stroke and its risk factors, 1990-2021: a systematic analysis for the Global Burden of Disease Study 2021. *Lancet Neurol*. 2024;23(10):973–1003. doi:10.1016/S1474-4422(24)00369-7
2. Chen RL, Balami JS, Esiri MM, Chen LK, Buchan AM. Ischemic stroke in the elderly: an overview of evidence. *Nat Rev Neurol*. 2010;6(5):256–265. doi:10.1038/nrneurol.2010.36
3. Boehme M, Guzzetta KE, Bastiaanssen TFS, et al. Microbiota from young mice counteracts selective age-associated behavioral deficits. *Nat Aging*. 2021;1(8):666–676. doi:10.1038/s43587-021-00093-9
4. Lan Y, Zhang X, Liu S, et al. Fate mapping of Spp1 expression reveals age-dependent plasticity of disease-associated microglia-like cells after brain injury. *Immunity*. 2024;57(2):349–363.e349. doi:10.1016/j.immuni.2024.01.008
5. Gao C, Jiang J, Tan Y, Chen S. Microglia in neurodegenerative diseases: mechanism and potential therapeutic targets. *Signal Transduct Target Ther*. 2023;8(1):359. doi:10.1038/s41392-023-01588-0
6. Colton C, Wilcock DM. Assessing activation states in microglia. *CNS Neurol Disord Drug Targets*. 2010;9(2):174–191. doi:10.2174/187152710791012053
7. Colton CA. Heterogeneity of microglial activation in the innate immune response in the brain. *J Neuroimmune Pharmacol*. 2009;4(4):399–418. doi:10.1007/s11481-009-9164-4
8. Amato S, Arnold A. Modeling microglia activation and inflammation-based neuroprotectant strategies during ischemic stroke. *Bull Math Biol*. 2021;83(6):72. doi:10.1007/s11538-021-00905-4
9. Zhang W, Tian T, Gong SX, et al. Microglia-associated neuroinflammation is a potential therapeutic target for ischemic stroke. *Neural Regen Res*. 2021;16(1):6–11. doi:10.4103/1673-5374.286954
10. Marino Lee S, Hudobenko J, McCullough LD, Chauhan A. Microglia depletion increase brain injury after acute ischemic stroke in aged mice. *Exp Neurol*. 2021;336:113530. doi:10.1016/j.expneurol.2020.113530
11. Suenaga J, Hu X, Pu H, et al. White matter injury and microglia/macrophage polarization are strongly linked with age-related long-term deficits in neurological function after stroke. *Exp Neurol*. 2015;272:109–119. doi:10.1016/j.expneurol.2015.03.021
12. Li T, Zhao J, Xie W, et al. Specific depletion of resident microglia in the early stage of stroke reduces cerebral ischemic damage. *J Neuroinflammation*. 2021;18(1):81. doi:10.1186/s12974-021-02127-w
13. Hou K, Li G, Yu J, Xu K, Wu W. Receptors, channel proteins, and enzymes involved in microglia-mediated neuroinflammation and treatments by targeting microglia in ischemic stroke. *Neuroscience*. 2021;460:167–180. doi:10.1016/j.neuroscience.2021.02.018
14. López-Otín C, Blasco MA, Partridge L, Serrano M, Kroemer G. Hallmarks of aging: an expanding universe. *Cell*. 2023;186(2):243–278. doi:10.1016/j.cell.2022.11.001
15. Yu S, Fu J, Wang J, et al. The influence of mitochondrial-DNA-driven inflammation pathways on macrophage polarization: a new perspective for targeted immunometabolic therapy in cerebral ischemia-reperfusion injury. *Int J Mol Sci*. 2021;23(1):135. doi:10.3390/ijms23010135
16. Reichner JS, Mulligan JA, Bodenheimer HC Jr. Electron transport chain activity in normal and activated rat macrophages. *J Surg Res*. 1995;59(6):636–643. doi:10.1006/jsre.1995.1217
17. Augusto-Oliveira M, Arrifano GP, Lopes-Araújo A, et al. What do microglia really do in healthy adult brain? *Cells*. 2019;8(10):1293. doi:10.3390/cells8101293
18. Tian Y, Zhu P, Liu S, et al. IL-4-polarized BV2 microglia cells promote angiogenesis by secreting exosomes. *Adv Clin Exp Med*. 2019;28(4):421–430. doi:10.17219/acem/91826
19. Wu TW, Liu CC, Hung CL, et al. Genetic profiling of young and aged endothelial progenitor cells in hypoxia. *PLoS One*. 2018;13(4):e0196572. doi:10.1371/journal.pone.0196572
20. Ma Q, Li R, Wang L, et al. Temporal trend and attributable risk factors of stroke burden in China, 1990-2019: an analysis for the Global Burden of Disease Study 2019. *Lancet Public Health*. 2021;6(12):e897–e906. doi:10.1016/S2468-2667(21)00228-0
21. Ergul A, Alhusban A, Fagan SC. Angiogenesis: a harmonized target for recovery after stroke. *Stroke*. 2012;43(8):2270–2274. doi:10.1161/STROKEAHA.111.642710

22. Cai M, Zhang W, Weng Z, et al. Promoting neurovascular recovery in aged mice after ischemic stroke - prophylactic effect of omega-3 polyunsaturated fatty acids. *Aging Dis*. 2017;8(5):531–545. doi:10.14336/AD.2017.0520
23. Yang GY, Jin K, Wang Y, et al. Ischemia-induced angiogenesis is attenuated in aged rats. *Aging and Disease*. 2016;7.
24. Chen Z, Xin L, Yang L, et al. Butyrate promotes post-stroke outcomes in aged mice via interleukin-22. *Exp Neurol*. 2023;363:114351. doi:10.1016/j.expneurol.2023.114351
25. Hudobenko J, Ganesh BP, Jiang J, et al. Growth differentiation factor-11 supplementation improves survival and promotes recovery after ischemic stroke in aged mice. *Aging*. 2020;12(9):8049–8066. doi:10.18632/aging.103122
26. Jiang L, Mu H, Xu F, et al. Transcriptomic and functional studies reveal undermined chemotactic and angiostimulatory properties of aged microglia during stroke recovery. *J Cereb Blood Flow Metab*. 2020;40(1_suppl):S81–S97. doi:10.1177/0271678X20902542
27. Shi L, Rocha M, Zhang W, et al. Genome-wide transcriptomic analysis of microglia reveals impaired responses in aged mice after cerebral ischemia. *J Cereb Blood Flow Metab*. 2020;40(1_suppl):S49–S66. doi:10.1177/0271678X20925655
28. Mossad O, Batut B, Yilmaz B, et al. Gut microbiota drives age-related oxidative stress and mitochondrial damage in microglia via the metabolite N (6)-carboxymethyllysine. *Nat Neurosci*. 2022;25(3):295–305. doi:10.1038/s41593-022-01027-3
29. Willenborg S, Sanin DE, Jais A, et al. Mitochondrial metabolism coordinates stage-specific repair processes in macrophages during wound healing. *Cell Metab*. 2021;33(12):2398–2414.e2399. doi:10.1016/j.cmet.2021.10.004
30. Hayakawa K, Okazaki R, Morioka K, Nakamura K, Tanaka S, Ogata T. Lipopolysaccharide preconditioning facilitates M2 activation of resident microglia after spinal cord injury. *J Neurosci Res*. 2014;92(12):1647–1658. doi:10.1002/jnr.23448
31. Ballout N, Rochelle T, Brot S, et al. Characterization of inflammation in delayed cortical transplantation. *Front Mol Neurosci*. 2019;12:160. doi:10.3389/fnmol.2019.00160